Marine Micropaleontology 79 (2011) 67–79

Contents lists available at ScienceDirect

Marine Micropaleontology

journal homepage: www.elsevier.com/locate/marmicro

Research paper

Paleoceanography of the Mauritanian margin during the last two climatic cycles: From planktonic foraminifera to African climate dynamics

K.M.R. Matsuzaki [a,1], F. Eynaud [a,*], B. Malaizé [a], F.E. Grousset [a,b], A. Tisserand [a,2], L. Rossignol [a], K. Charlier [a], E. Jullien [a]

[a] Laboratoire EPOC UMR/CNRS 5805, Université Bordeaux 1, Avenue des Facultés, F-33405 Talence, France
[b] Observatoire Aquitain des Sciences de l'Univers, Floirac, France

ARTICLE INFO

Article history:
Received 31 May 2010
Received in revised form 25 January 2011
Accepted 26 January 2011

Keywords:
NW African margin
Planktonic foraminifera
Sea-surface salinity
African monsoons
Late Pleistocene

ABSTRACT

The last 220 ka of the MD03-2705 (18° 05.81′ N–21° 09.19′ W) sedimentary sequence, retrieved off the Cape Verde islands, was investigated using a multiproxy approach. Planktonic foraminifera assemblage analyses, coupled with isotopic measurements ($\delta^{18}O$) from benthic (*Planulina wuellerstorfi*) and planktonic (*Globigerinoides ruber*) foraminifera monospecific samples were conducted along the topmost 11 m of the sequence. High resolution X-ray fluorescence measurements (0.5 cm resolution), giving access to major element ratio, have completed the geochemical analyses along the core. Seasonal and annual past sea surface temperatures (SST) were quantitatively reconstructed. Local sea-surface salinity (SSS) changes were then estimated by coupling SST with planktonic $\delta^{18}O$ data. Our data provide a set of both oceanic and continental markers of environmental changes along the north-western African margin. The major changes detected in our record are discussed in the light of the regional paleoceanographic and paleoclimatic history of the last 220 ka. Coupled oceanographic and atmospheric processes portray the climatic evolution of the area, and show strong links among the regional oceanography (water mass advection), the upwelling dynamics and the Intertropical Convergence Zone (ITCZ) migration. An increased upwelling activity (or influence of upwelling filaments) is noted at the end of the two last glacial periods, probably in response to a more southerly position of the ITCZ. Higher SSS are recorded over the area during arid intervals and were tentatively interpreted as signing a southward shift of the Cape Verde Frontal Zone. A detailed coupling between dust advection and SSS values over the site of study was noted during MIS6.5.

1. Introduction

Climatic processes which characterise the north-western African region illustrate well the interplay of the oceanic, atmospheric and land reservoirs along both latitudinal and longitudinal gradients. The climate of this area is actually driven by the seasonal displacement of the Intertropical Convergence Zone (ITCZ), with the accompanying migration of dry and intense trade winds, which implies drastic semi-annual changes on the continent and the adjacent ocean. Intense precipitation generally accompanies the ITCZ migration. This mechanism, complemented by the heat difference between the Sahara and the Equatorial Atlantic, is called the West African Monsoon (WAM, e.g. Chang et al., 1997; Hall and Peyrillé, 2006). Meteorological links between these phenomena have however recently been questioned (Nicholson, 2009), suggesting that the ITCZ should be distinguished from the "tropical rainbelt". According to Nicholson (2009), rainfall in the region is driven by features in the upper-level circulation rather than by surface features themselves (i.e. the ITCZ and moist southwest "monsoon" flow). Nicholson (2009) further suggests that the ITCZ definition itself should be revised, because it is biassed by the definition of the Atlantic marine ITCZ (i.e., a surface zone of convergence that produces ascent and intense convection), while the structure of the equatorial convergence zone over West Africa is quite different.

At the scale of Quaternary climatic oscillations, it has been suggested that the general southward displacement of the ITCZ during glacial periods and especially during high-latitude iceberg-discharges known as Heinrich events (HE) might have had a drastic impact on the continental aridity of the Sahara and Sahel regions (Tiedemann et al., 1989; Tiedemann, 1991; deMenocal, 1995, 2004; Broccoli et al., 2006; Mulitza et al., 2008; Itambi et al., 2009; Niedermeyer et al., 2009) and also on the dynamics of the eastern

* Corresponding author. Tel.: +33 5 4000 3319; fax: +33 5 4000 0848.
E-mail addresses: k.m.matsuzaki@gmail.com (K.M.R. Matsuzaki), f.eynaud@epoc.u-bordeaux1.fr (F. Eynaud), b.malaize@epoc.u-bordeaux1.fr (B. Malaizé), f.grousset@epoc.u-bordeaux1.fr (F.E. Grousset), amandine.tisserand@bjerknes.uib.no (A. Tisserand), l.rossignol@epoc.u-bordeaux1.fr (L. Rossignol), k.charlier@epoc.u-bordeaux1.fr (K. Charlier).
[1] Present address: C/O Department of Geoenvironmental Science, The Center for Academic Resources and Archives, Tohoku University Museum, Tohoku University, Aramaki Aza Aoba 6-3, Aoba-ku, Sendai, 980-8578, Japan.
[2] Now at Bjerknes Centre for Climate Research, Bergen, Norway.

0377-8398/$ – see front matter © 2011 Elsevier B.V. All rights reserved.
doi:10.1016/j.marmicro.2011.01.004

boundary upwelling systems off Africa (i.e. Mittelstaedt, 1983, 1991; Thiede, 1975, 1983; Prell and Curry, 1981; Ganssen and Sarnthein, 1983; Wefer et al., 1983; Prell, 1984; Sarnthein et al., ; Martinez et al., 1999). Resulting eolian dust fluxes to the ocean were deeply modified during these large amplitude climatic shifts (e.g. Sarnthein and Koopman, 1980; Jullien et al., 2007; Mulitza et al., 2008; Itambi et al., 2009). Most of the data regarding African paleoclimate were obtained from marine cores retrieved off Mauritania. Here we present results from the analysis of the first 11 m of the core MD03-2705 (18° 05.81′ N; 21° 09.19′ W). This core, retrieved between the Cape Blanc and the Cape Verde (Fig. 1), already provided important insights regarding the regional climatic variability of the last (Jullien et al., 2007) and penultimate (Tisserand et al., 2009) glacial periods. Strong links between subtropical climates and north-hemispheric forcings were especially underlined at millennial scale (e.g. Jullien et al., 2007).

The present study offers a detailed and continuous record of sea-surface conditions over the last two climatic cycles, primarily derived from the analyses of planktonic foraminifera assemblages. To highlight sea-surface hydrological changes and test their link with the migration of the ITCZ, the upwelling dynamics and the evolution of the African monsoons, we have integrated benthic and planktonic stable isotope ($\delta^{18}O$) data, and major element ratio obtained by X-ray fluorescence (XRF). Taken together, these proxies provide a set of both oceanic and continental markers of regional environmental change over the last 220 ka. We have also reconstructed seasonal and annual past sea surface temperature (SST) using planktonic foraminifera transfer functions, which, coupled to the planktonic stable ^{18}O record, allowed us to evaluate past sea-surface salinity change.

This paper discusses the most salient features detected throughout our record, with a special consideration to glacial periods. Ocean dynamics (including upwelling) are discussed in connection to atmospheric circulation in the light of tropical and polar teleconnections.

2. Environmental setting

2.1. Modern climatic setting

The core MD03-2705 was retrieved in a modern "oceanic dust spot", an area where atmospheric dust concentration (inferred from mean annual equivalent aerosol optical depth, Husar et al., 1997) is among the strongest, with modern global fluxes of mineral aerosols to the ocean higher than 10^3 mg m^{-2} $year^{-1}$ (e.g. Harrison et al., 2001).

Modern climate over the north-western (NW) African margin is governed by monsoonal dynamics: the West Africa monsoon (WAM). Up to the recent revision of Nicholson (2009), the WAM dynamics was classically associated with seasonal latitudinal shifts of the ITCZ (Fig. 1). Nicholson (2009) suggested a more complex pattern, especially for the boreal summer situation, in which the ITCZ is only a component of the system. However, basic forcing remains the same, i.e., the seasonal meridional displacement of the climatic belts.

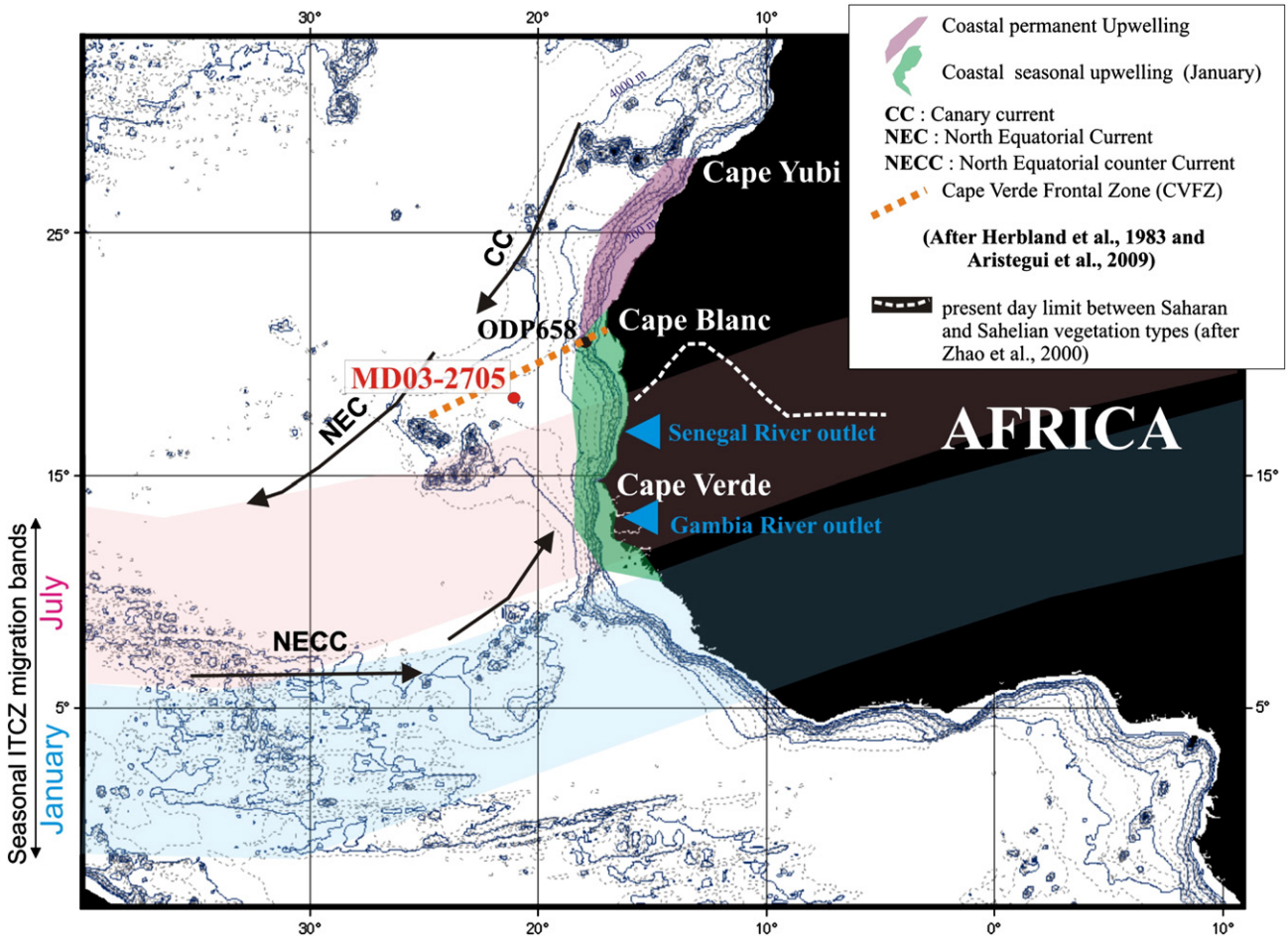

Fig. 1. Location of the studied core MD03-2705 along the north-western African margin compared with the atmospheric and oceanographic regional settings. Black arrows schematize the pathway of the modern dominant surface currents in the area, with CC = Canary Current, NEC = North Equatorial Current, NECC = North Equatorial Counter Current. The coastal purple zone delimits the modern permanent upwelling area, and the green one the seasonal upwelling area. The dotted orange line marks the position of the modern Cape Verde Frontal Zone (CVFZ) (after Herbland et al., 1983; Aristegui et al., 2009). Red and blue bands respectively identify the migration domains of the summer and winter Intertropical Convergence Zone (ITCZ). The position of the ODP658 record (deMenocal et al., 2000a,b) is indicated.

(i) In winter, the equatorward displacement of the ITCZ (5° N) causes a southward shift of dry subtropical air masses and is associated with the development of strong easterly Saharan Air Layer (SAL) winds. The southward shift of the ITCZ and wind development (especially Harmattan, Tulet et al., 2008) causes dust transport from the Sahara. The dust plume is generally located between 15 and 25° N along an E–W axis over the tropical Atlantic Ocean (Holz, 2004).
(ii) During boreal summer, dry subtropical air is shifted northward as the ITCZ is located around 20° N (Fig. 1). It represents the onset of the rainy season (summer monsoon) with heavy rainfall and changes in atmospheric circulation (Peyrillé et al., 2007). Trade winds from the southern hemisphere, loaded with water vapour over the Gulf of Guinea, penetrate the West African continent far to the north. The moisture-laden air spreads over ocean and continent, permitting heavy rains over West Africa. Nicholson (2009) suggested that three quasi-independent mechanisms control precipitation development over West Africa in summer: ascent of air masses linked to the upper-level jet streams, convergence associated with the surface ITCZ, and a coastal circulation cell linked to sea-breeze effects.

Complex parameters and mechanisms actually modulate precipitation. Surface temperature anomalies of adjacent oceanic basins could also balance the northward expansion of the monsoon, primarily by changes in the evaporation budget. Among the important oceanic basins, are the Gulf of Guinea, as previously introduced, and the Mediterranean Sea, from which a warming could favour the northward penetration of the monsoon in summer (Rowell, 2003; Hall and Peyrillé, 2006; Peyrillé et al., 2007; Fontaine et al., 2009). The role of sea-surface temperatures was also supported by Nicholson (2009), who however suggested that the accompanying surface pressure gradient could constitute a further causal mechanism for Sahel rainfall modulation.

2.2. Oceanographic setting

As part of the Eastern Boundary Current (EBC) system, the NW African margin is one of the main upwelling areas in the Atlantic Ocean (Aristegui et al., 2009). Along the NW African margin, the temporal dynamics of the upwelling is basically controlled by the intensity of trade-winds, itself dependent of the seasonal ITCZ migration (e.g. Mittelstaedt, 1991; Hagen, 2001; Stramma et al., 2005). As a result, the Senegalo-Mauritanian waters display the highest seasonal SST variance of the tropical Atlantic (Faye et al., 2009).

Two domains are distinguishable in latitude (Fig. 1): (1) the area off Cape Blanc is dominated by permanent upwelling (namely the Mauritanian upwelling), while (2) the area located a little further south, off Cape Verde, is under the influence of seasonal upwelling prevalent from November to February, i.e., in winter (e.g. Herbland et al., 1983). If satellite imagery indicates that upwelling and productive area are at present mainly located over the shelf (Van Camp et al., 1991), previous studies have however demonstrated that sediments deposited for long time over the slope are good candidates to document past variations of productivity (Martinez et al., 1999).

The studied area (Fig. 1) is under the influence of the major return branch of the subtropical gyre, the Canary Current (CC), flowing southward along the north-west African coast to 15° N, then turning west to form the North Equatorial Current (NEC) (Stramma and Siedler, 1988; Klein and Siedler, 1989; Barton et al., 1998; Stramma et al., 2005; Hernandez-Guerra et al., 2005; Aristegui et al., 2009). The average CC consists of a southwestward mass transport of 3.0 to 4.0 Sv (Hernandez-Guerra et al., 2005), carrying temperate/subpolar waters along the south-western European margin to the West African coast on a large seasonal variability. The spatially averaged CC flow is maximal during winter when the subtropical gyre is located further north (29° N in winter versus 27° N in summer) and further offshore (e.g. Navarro-Pérez and Barton, 2001).

A current of opposite direction to the CC is the North equatorial counter current (NECC), which flows intermittently in the area and transports water with low salinity and high nutrient concentration along the coast of Mauritania (Fig. 1). This current is highly variable and disappears from November to January (Richardson and McKee, 1984; Gouriou, 1993).

Surface water masses of either northern (North Atlantic Central Waters, NACW) or southern (South Atlantic Central Waters, SACW) origin are delineated by the Cape Verde Frontal Zone (CVFZ). The CVFZ is located at about 20° N off Africa oriented south-westward to about 16° N in the central tropical Atlantic (Fig. 1). The front is associated with a convergence at the coast between the Canary Current conveying NACW southward and a northward flow of SACW (e.g. Hernandez-Guerra et al., 2005; Stramma et al., 2005; Aristegui et al., 2009).

Below the surface, the water column is structured by two main water masses: (1) Intermediate waters are characterised by the confluence of Antarctic Intermediate Waters (AAIW, in the 600–1000 m range) coming from the south, with Mediterranean (MW) and Arctic Intermediate Waters (AIW, down to nearly 1500 m, Knoll et al., 2002; Llinas et al., 2002) coming from the north. Our area represents the septentrional limit of the AAIW influence at present (Knoll et al., 2002). (2) In deep-waters, Sarnthein et al. (1982) distinguished the North Atlantic Deep Water (NADW) flowing southward (between 1700 and 4000 m) and saturated in carbonate, from the corrosive Antarctic Bottom Water (AABW) below 4000 m.

3. Materials and methods

Our study was focussed on the core MD03-2705, retrieved from the northeastern margin of the Cape Verde islands at 3085 m water depth (Fig. 1), during the MD134-PICABIA cruise (RV Marion Dufresne II, Turon and Malaizé, 2003). The coring site is located at the submarine terrace of Cape Verde, 450 km off the Mauritanian coastline and elevated approximately at 300 m above the abyssal plain. The sedimentation in the area is likely hemipelagic to pelagic, with no perturbations by the arrival of reworked material via gravity flows (Weaver et al., 2000; Holz, 2004). The biogenic fraction is mainly composed of a foraminifera and nannoplankton ooze. However, the MD03-2705 site is under the influence of dust plumes from the continent (deMenocal et al., 2000a,b; Jullien et al., 2007; Tisserand et al., 2009; Itambi et al., 2009). Previous works conducted on the core MD03-2705 provided a continuous record of the composition of minor/trace elements derived from the scan of bulk sediments using the Bremen X-ray fluorescence (XRF)-Cortex facility (measurement resolution: 0.5 to 1 cm, Jullien et al., 2007). For this paper, we used the Ti/Al ratio, considered as a good proxy of wind intensity (e.g. Boyle, 1983; Rea, 1994) along the West African margin (Jullien et al., 2007; Tisserand et al., 2009; Itambi et al., 2009).

Our analyses are primarily based on planktonic foraminifera, associating paleoecological (assemblages) and geochemical (stable isotopes) approaches. 173 samples were analysed for faunal assemblages of planktonic foraminifera. These analyses have been conducted every 10 cm at the lowest resolution up to every 2 cm in some sections (MIS2 to MIS4). Samples of roughly 4 to 5 cm^3 of dry sediment were washed through a 150-μm sieve. The coarse fraction (>150 μm) was dried overnight, weighted and then split with a microsplitter for analyses of planktonic foraminifera assemblages. Due to the high diversity in this tropical area, counts were made on a mean population of 450 specimens (minimum of 277 and maximum of 911 specimens). Species-level identification followed the compilation of Hemleben et al. (1989) and Kennett and Srinivasan (1983).

Relative abundances of species were used to perform quantification of Sea Surface Temperatures (SST) thanks to an ecological transfer function (Guiot and de Vernal, 2007) developed at EPOC ("Environnements et Paléoenvironnement OCéaniques", Bordeaux1 University, France). The method used here is based on the Modern Analogue Techniques (MAT, e.g. Kucera, 2007) running under the R software using a script first developed for dinocyst transfer functions by Guiot and Brewer (www.cerege.fr/IMG/pdf/formationR08.pdf). The modern database used is derived from the ones developed separately for the North Atlantic and the Mediterranean Sea during the MARGO project (Kucera et al., 2005; Hayes et al., 2005). These databases were merged to offer a larger set of analogues for subtropical reconstructions over the last glacial period notably (Eynaud, unpublished data): 1007 points are then compiled and modern hydrological parameters were requested from the WOA (1998) database using the tool developed by Schaffer-Neth during the MARGO project (http://www.geo.uni-bremen.de/geomod/Sonst/Staff/csn/woasample.html). This method permits the reconstruction of annual and seasonal SST (average winter, spring, summer and fall) with a degree of confidence (root mean square error) of 1.1 °C for Spring and Annual SST, 1.2 °C for Winter and Fall SST, and 1.3 °C for Summer SST (Eynaud, unpublished data). Calculations of past hydrological parameters rely on a weighted average of SST values from the best five modern analogues, with a maximum weight given for the closest analogue in terms of statistical distance, i.e., dissimilarity minimum (e.g. Kucera et al., 2005; Guiot and de Vernal, 2007).

Stable isotopic analyses were performed at EPOC, using an Optima Micromass mass spectrometer (see Jullien et al., 2007; Tisserand et al., 2009). For each measurement, 80 μg mean weight aliquots (8 to 10 specimens of the planktonic species *Globigerinoides ruber* (white), and 4 to 6 specimens of the benthic species *Planulina wuellerstorfi*) were treated with individual acid baths. The extracted CO_2 gas was analysed versus a laboratory reference gas calibrated with respect to VPDB (for Vienna Pee Dee Belemnite), using the international standard NBS 19. Standard deviations of multiple replicate measurements of this standard are ± 0.06 (1σ) per mil for $\delta^{18}O$ measurements on *G. ruber* (white), and ± 0.05 (1σ) per mil for $\delta^{18}O$ measurements on *P. wuellerstorfi*. Multiple analyses (duplicates or triplicates) were performed at each level, to reduce external uncertainties. The pooled standard deviation of replicates are ± 0.21 (1σ) per mil for $\delta^{18}O$ measurements respectively on *G. ruber* (white), and ± 0.19 ($1\ \sigma$) per mil for $\delta^{18}O$ measurements of *P. wuellerstorfi*.

$\delta^{18}O$ data obtained on the planktonic foraminifera *G. ruber* (white) along the core MD03-2705 were combined with SST reconstructions to estimate the sea-surface salinity (SSS) changes using the method discussed in Malaizé and Caley (2009). To estimate past sea-surface salinity variations, we have evaluated changes in the $\delta^{18}O$ of the sea water ($\delta^{18}Osw$), as long as both have been quantitatively related by calibrations proposed by Craig and Gordon (1965). Following Duplessy et al. (1991), we used the paleotemperature equation defined by Epstein et al. (1953), linking SST with both $\delta^{18}Osw$ and $\delta^{18}O$ of planktonic

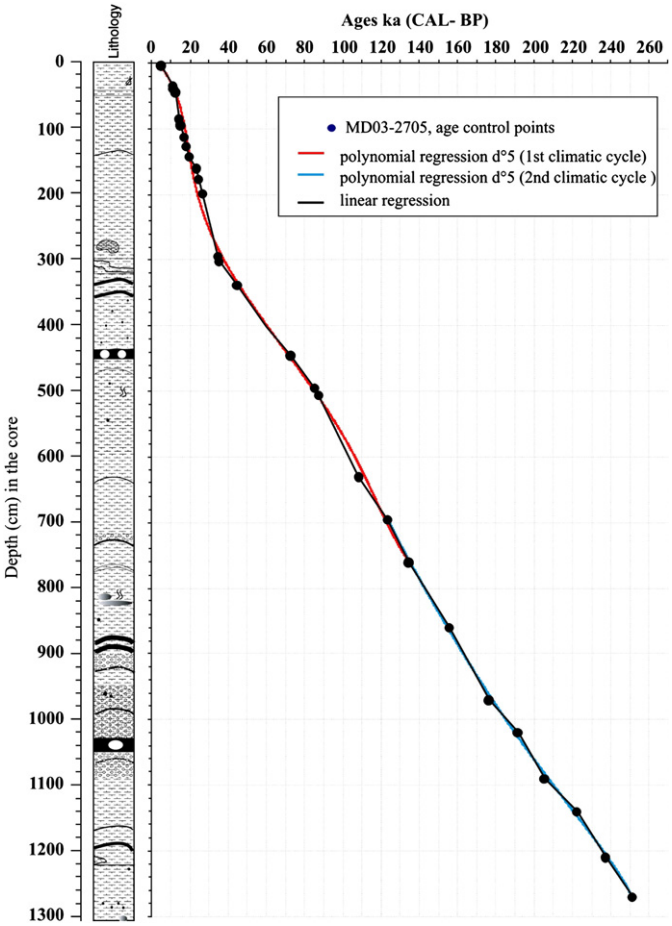

Fig. 2. The core MD03-2705 age model for the last 250 ka BP (see also Table 1). The age control points (black dots) conform to those used in Jullien et al. (2007) and Tisserand et al. (2009). Two polynomial regressions (d°5) were used to fit the pointers at the best. Polynomial regression for the last climatic cycle (red), and polynomial regression for the penultimate climatic cycle (blue). They are compared to the 28 linear regressions which were used in the case of a linear age model. The sedimentological description of the first 13 m of core MD03-2705 is plotted on the left (PICABIA cruise report, 2003).

foraminifera shells. For each sample, we used summer SST values derived from the ecological transfer function described previously, together with $\delta^{18}O$ measurements on *G. ruber*, to estimate past $\delta^{18}Osw$ values (uncertainty of 0.4‰). The calculated sea water $\delta^{18}O$ record depends not only on local salinity changes, but also on global oceanic $\delta^{18}O$ changes, linked to global continental ice volume variations during glacial–interglacial climatic changes. To estimate the local signal of these $\delta^{18}Osw$ changes, we retrieved the global effect using estimations of past global $\delta^{18}Osw$ changes (Waelbroeck et al., 2002).

Previous works have presented quantitative reconstructions of past SSS (e.g. Duplessy et al., 1991; Maslin et al., 1995; Flower et al., 2004), based on modern relationships between local $\delta^{18}O$ sea water and local sea surface salinities (Craig and Gordon, 1965; Ostlund et al., 1987). Meanwhile, some authors recently stressed the importance of uncertainties involved in such quantitative estimations. These uncertainties are linked to strong discrepancies observed for the spatial $\delta^{18}O$–SSS relationships of different oceanic areas (Schmidt, 1999; LeGrande and Schmidt, 2006), or linked to temporal changes in the end-members of these $\delta^{18}O$–SSS relationships, especially during such drastic climatic changes as glacial–interglacial transitions (Rohling and Bigg, 1998; Rohling, 2000). According to these studies, error propagation in past SSS calculations is too large to allow accurate quantitative reconstruction in most oceanographic provinces. Following their recommendations, we have decided to use here only the residual $\delta^{18}O$ signal as a qualitative estimate of past SSS changes.

4. Chronology

The stratigraphy of core MD03-2705 is based on 8 AMS-^{14}C dates obtained on monospecific samples of the planktonic foraminifera *Globigerina bulloides* (>150 μm), for the top-most part of the core (Jullien et al., 2007). Beyond the range of AMS ^{14}C ages, the age model is based on the correlation of the benthic $\delta^{18}O$ record (*P. wuellerstorfi*, after Jullien et al., 2007; and Tisserand et al., 2009) with the $\delta^{18}O$ LR04Stack (Lisiecki and Raymo, 2005) and the $\delta^{18}O$ record obtained by deMenocal et al. (2000b) on the proximal core ODP-658C (see

Table 1
Age control points used to build the chronology of the first 1270 cm of the core MD03-2705 after Jullien et al. (2007) and Tisserand et al. (2009).

Depth (cm)	Corrected ^{14}C ages (ka)	Standard error	Calibration two sigma ranges after Stuiver et al. (2005) (cal yr BP)	Calendar ages (ka)	Source
3	4.38	40	5040–5300	5.190	AMS-^{14}C dating,
34	10		11,370–11,910	11.600	Microfaunal event (*G. menardii*) in Jullien et al. (2007)
38	10.15	70	11,690–12,310	11.780	AMS-^{14}C dating, in Jullien et al. (2007)
44	10.6		12,670–12,840	12.740	Isotopic event (tuned on ODP-658C after deMenocal et al., 2000b) in Jullien et al. (2007)
85	12.46		14,255–15,063	14.720	Microfaunal event (*G. inflata*) in Jullien et al. (2007)
94	13.01	80	15,150–15,880	15.490	AMS-^{14}C dating, Jullien et al. (2007)
112	14.38	40	16,970–17,800	17.310	AMS-^{14}C dating, Jullien et al. (2007)
126	14.95		18,430–18,680	18.500	Isotopic and Microfaunal event (*G. inflata*) in Jullien et al. (2007)
142	16.74	60	19,840–20,160	19.980	AMS-^{14}C dating, Jullien et al. (2007)
160	19.8	100	23,490–24,160	23.840	AMS-^{14}C dating, Jullien et al. (2007)
176	21.21	120		24.990	AMS-^{14}C dating, calibration after Bard (1998), in Jullien et al. (2007)
198				27.000	Isotopic events 3.0 after Lisiecki and Raymo (2005); Jullien et al. (2007)
294				35.000	$\delta^{13}C$ Isotopic event (tuned on core SU90-08 after Vidal et al., 1998) in Jullien et al. (2007)
302	30.77	350		35.820	AMS-^{14}C dating, calibration after Bard (1988), in Jullien et al. (2007)
338				45.000	$\delta^{13}C$ Isotopic event (tuned on core SU90-08 after Vidal et al., 1998) in Jullien et al. (2007)
445				73.000	Isotopic events 5.0 after Lisiecki and Raymo (2005); Jullien et al. (2007)
495				85.550	Isotopic events: transition 5.2 to 5.1 after Lisiecki and Raymo (2005); Jullien et al. (2007)
505				88.030	Isotopic events 5.2 after Lisiecki and Raymo (2005); Jullien et al. (2007)
630				109.000	Isotopic events 5.4 after Lisiecki and Raymo (2005), in Tisserand et al. (2009)
695				124.000	Isotopic events 5.5 after Lisiecki and Raymo (2005) in Tisserand et al. (2009)
725				132.500	Isotopic events 6.1–5.5 after Lisiecki and Raymo (2005); Jullien et al. (2007)
760				135.000	Isotopic events 6.2 after Lisiecki and Raymo (2005), in Tisserand et al. (2009)
860				156.000	Isotopic events 6.4 after Lisiecki and Raymo (2005), in Tisserand et al. (2009)
970				177.000	Isotopic events 6.5 after Lisiecki and Raymo (2005), in Tisserand et al. (2009)
1020				192.000	Isotopic events: 7.1–6.6 transition after Lisiecki and Raymo (2005), in Tisserand et al. (2009)
1090				206.000	Isotopic events 7.2 after Lisiecki and Raymo (2005), in Tisserand et al. (2009)
1140				223.000	Isotopic events 7.4 after Lisiecki and Raymo (2005), in Tisserand et al. (2009)
1210				238.000	Isotopic events 7.5 after Lisiecki and Raymo (2005), in Tisserand et al. (2009)
1270				252.000	Isotopic events 8.2 after Lisiecki and Raymo (2005), in Tisserand et al. (2009)

Fig. 1). 23 tie points are then generated in between 3 and 1270 cm depth in the core (see Fig. 2; Table 1 and Jullien et al., 2007; and Tisserand et al., 2009 for a detailed review of the age model construction). Two polynomial regressions (d°5) were used for the best fit of tie-points, and to avoid artificial breaks due to linear interpolation (Fig. 2).

5. Results

5.1. Planktonic foraminifera assemblages

Up to 30 species were recognised in the core with a mean species number of 22 per sample. Dominant species are *Globorotalia inflata*, species of the *Pachyderma-Dutertrei* (PD) intergrade complex (with a large dominance of *Neogloboquadrina pachyderma* dextral), associated with *G. bulloides* (Fig. 3). These three species represent a minimum of 50% of the total assemblages. *G. ruber* (white and pink), and *Globigerinita glutinata* have a maximum relative abundance rarely higher than 10%. Minor species, which have a maximum relative abundance of 5%, or are present intermittently over the studied period, are *Orbulina universa*, *Globigerina calida*, *Globigerinoides trilobus*, *Globigerinoides sacculifer*, *Globigerinella siphonifera*, *Globorotalia truncatulinoides* (dextral and sinistral), *Globorotalia crassaformis*, *Globorotalia hirsuta* and *Globorotalia menardii*.

Relative abundances of *G. bulloides* vary from 5 to 30%. Depletions in relative abundances of this species (underlined by white bands in Fig. 3) are concomitant of those of *G. inflata*. Alternatively, thermophylous taxa as *G. ruber*, especially *G. ruber* (pink), *G. trilobus*, *G. menardii* (in red in Fig. 3) develop at that time.

5.2. An empirical view of the hydrological parameters over the last 220 ka

Fig. 4 compares the abundance of tropical species (sum of the taxa *G. trilobus*, *G. ruber* (white and pink), *G. sacculifer*, *G. menardii* and *O. universa* defined after Bé, 1977; Bé and Huston, 1977; Hemleben et al., 1989), quantitative reconstructions (annual, winter and summer SST) and stable isotope derived data (benthic and planktonic $\delta^{18}O$, and the residual $\delta^{18}O$ indicative of the salinity changes) over time.

In concordance with the isotope stratigraphy (Martinson et al., 1987; Lisiecki and Raymo, 2005), a threshold of 15% for tropical taxa could be used to define interglacial conditions (MIS7, 5 and 1, respectively). Abundance of the tropical assemblage, associated to SST close to their modern values, and low $\delta^{18}O$ values, characterise full interglacial

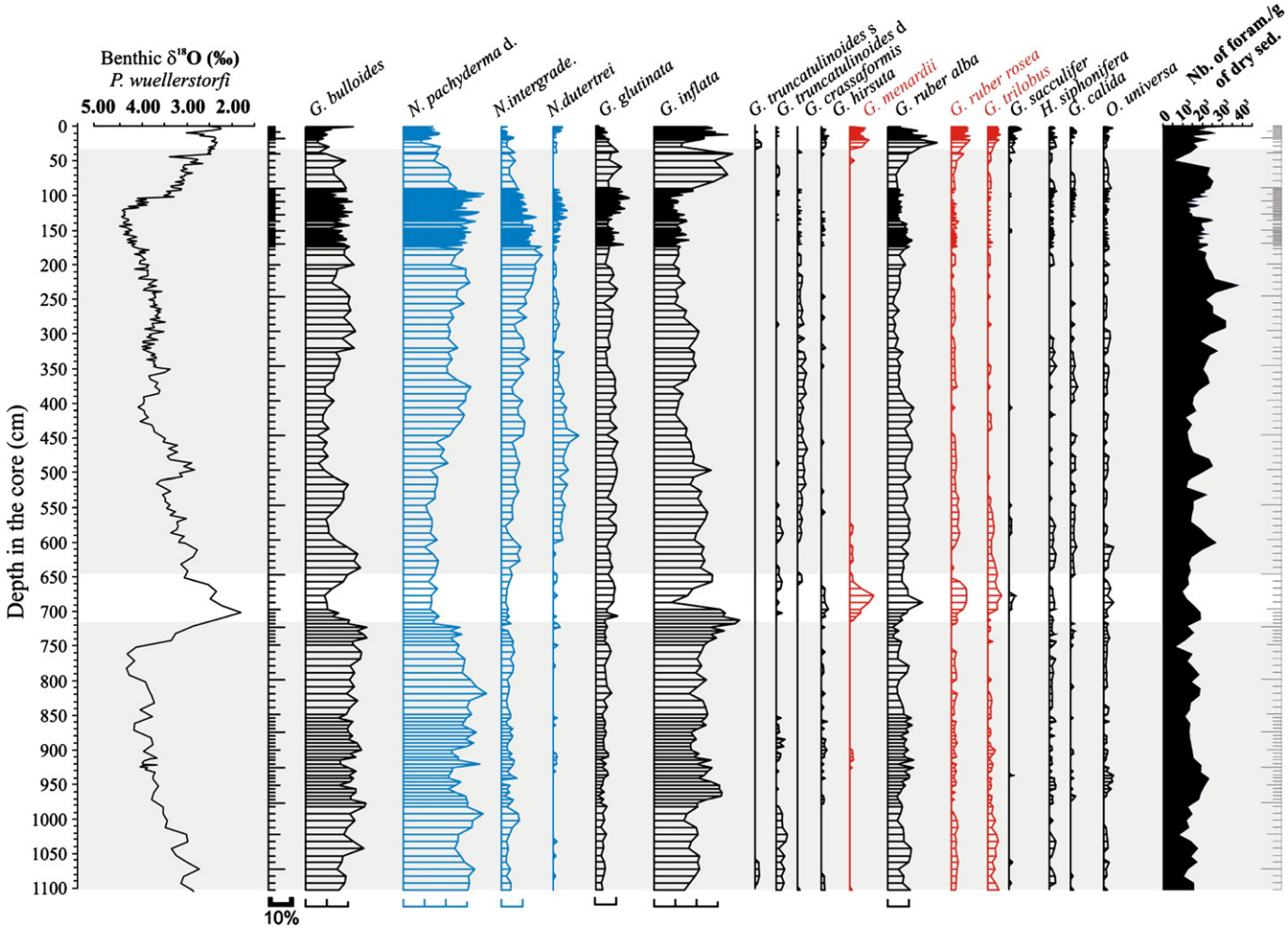

Fig. 3. Planktonic foraminifera assemblages (relative abundances of the most representative species) along the first eleven meters (0–1100 cm, the vertical scales bordering the diagram reflect sampling resolution) of core MD03-2705 compared to the benthic $\delta^{18}O$ data obtained on *P. wuellerstorfi*. Planktonic foraminifera absolute concentration (number of planktonic foraminifera per gramme of dry sediment) is depicted on the right side. The horizontal scale is given at the bottom of the diagram (10%, absence of scale for some species indicates abundances lower than 10%). Species in blue are those forming the PD intergrade complex and those in red are thermophylous species.

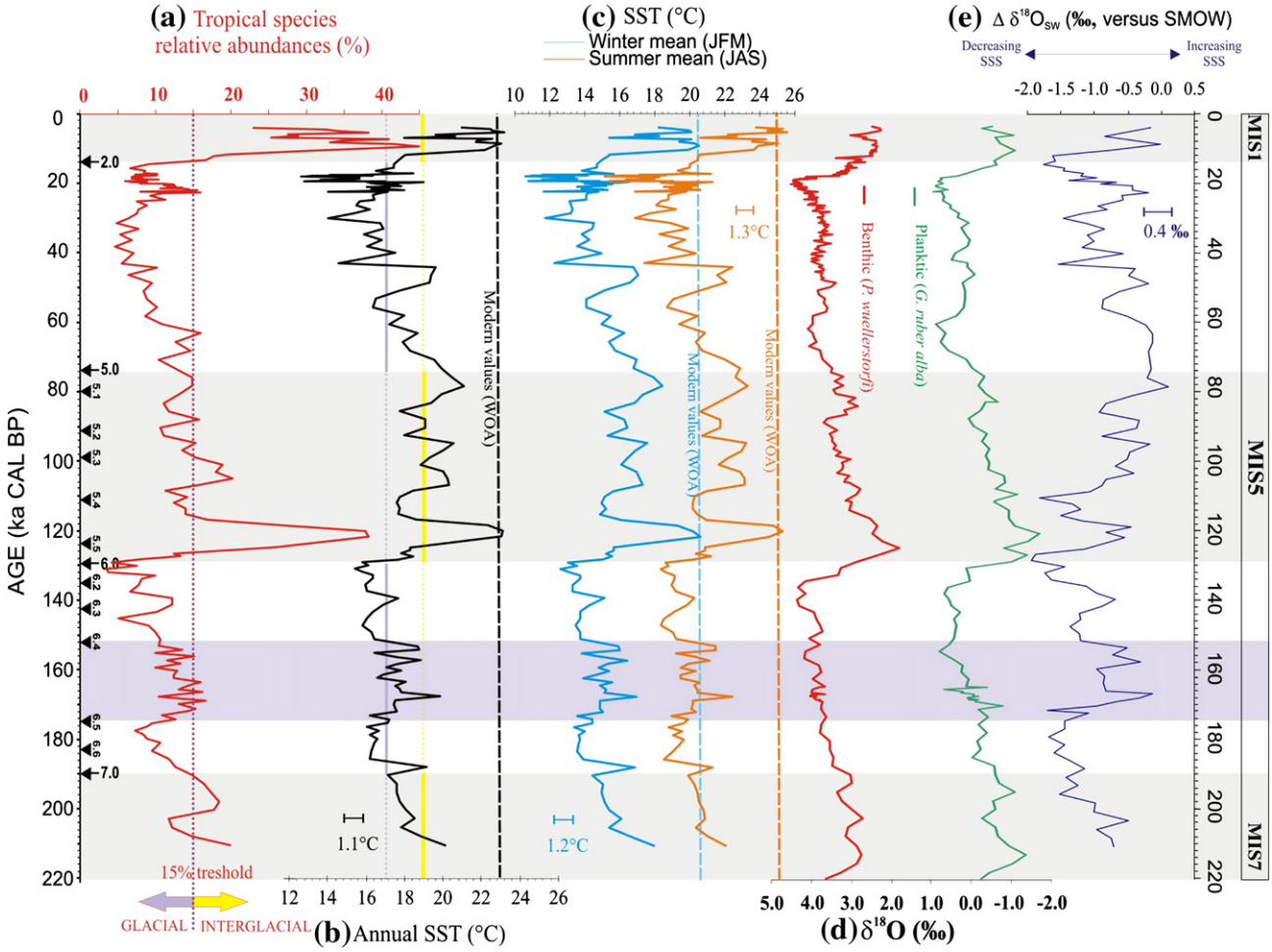

Fig. 4. Sea-surface conditions off Mauritania during the last 220 ka as documented by the abundance of tropical species (a: sum of the taxa *G. trilobus*, *G. ruber alba* and *rosea*, *G. sacculifer*, *G. menardii* and *O. universa* defined after Bé, 1977; Bé and Huston, 1977; Hemleben et al., 1989), quantitative reconstructions (b: mean annual SST, the blue and yellow lines refer respectively to the mean glacial and interglacial values; c: mean winter—JFM: January, February, March—and mean summer—JAS: July, August, September—SST) and the stable isotope derived data (d: benthic and planktonic $\delta^{18}O$, and e: the residual $\delta^{18}O_{SW}$ indicative of the local sea surface salinity changes). Modern values from WOA (1998). Grey bands delineate the warm interglacial periods (marine isotopic stages) and black arrows locate the major isotopic events after Martinson et al. (1987). The purple band underlines the MIS6.5 period.

conditions (MIS5.5 substage and the Holocene warming). Benthic isotopes range from glacial values of 4.5‰ to values of 2‰ during interglacial optima, whereas planktonic values obtained from *G. ruber* (white) reveal a glacial/interglacial shift from 0 to −2‰, respectively.

According to our results, the last 220 ka includes a large variability in sea-surface parameters. The reconstructed SSTs depict oscillations of various amplitudes throughout time which are statistically significant regarding the reconstruction error bar of maximum 1.3 °C for summer SST. Glacial annual SST values fluctuate around 17 °C (blue line in Fig. 4), whereas interglacial stages record mean SST of 19 °C (yellow line in Fig. 4). The seasonal values are globally 2 °C lower regarding the winter season and 2 °C higher for the summer months respectively. Largest shifts are recorded at the interglacial onsets/glacial terminations. Moreover, according to our quantifications, a warming of nearly 8 °C marks Terminations 2 and 1 (seen on annual and seasonal reconstructions). Glacial inceptions also record major, but somewhat more gradual changes in SST: for instance, an abrupt cooling of 5 °C is recorded for the 5.5 substage termination, whereas a gradual cooling of nearly 4 °C marks MIS7/MIS6 and MIS5/MIS4 transitions. Within glacials, a long term cooling characterises the installation of full glacial conditions during which annual SST could have been as low as 13 °C (i.e. at 18 ka, values of 11 °C for winter and 15 °C for summer). The amplitudes of these SST shifts are especially high considering the tropical location of the core, but are close to the ones detected by previous works in the area. For instance, deMenocal et al. (2000a) documented a SST anomaly up to 8 °C between the last glacial and the present.

6. Discussion

6.1. Long term trends over the last 220 ka BP: "a coupled ocean–continent response"

Following pioneering works of Boyle (1983) and Rea (1994), many paleoceanographic studies along the West African margin (e.g. Moreno et al., 2001; Jullien et al., 2007; Mulitza et al., 2008; Itambi et al., 2009; Tisserand et al., 2009) have used Titanium and Aluminium contents in sediments to monitor dust fluxes to the ocean, and their relation to periods of drought and/or wind strength on the continent. In our record, the Ti/Al ratio was used as a proxy of terrigenous material supplies from the African desert and according wind strength. High Ti/Al ratios were interpreted as reflecting higher dust supplies (Jullien et al., 2007; Tisserand et al., 2009). Fig. 5 compares this Ti/Al ratio to marine proxies of sea-surface conditions (SST, residual $\delta^{18}O$ as an indicator of SSS) obtained in core MD03-2705 over the last 220 ka. These data are integrated in a climatic frame defined after the works of deMenocal et al. (2000b), which have used the

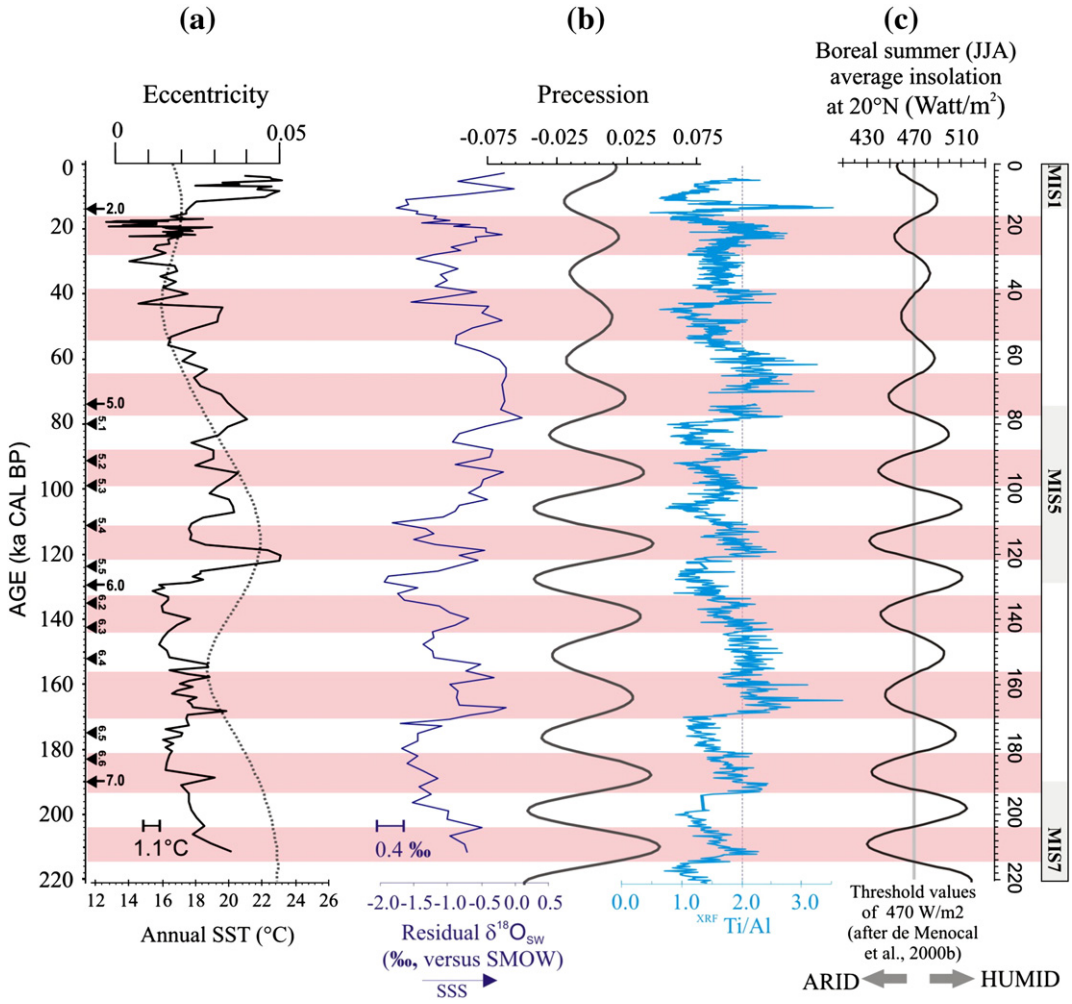

Fig. 5. Comparison of selected data from the core MD03-2705 to orbital parameters along the last 220 ka. (a): Eccentricity index versus annual SST; (b): precession index versus the residual $\delta^{18}O_{SW}$ and the Ti/Al ratio; (c): boreal summer (JJA) average insolation (generated at 20° N, after Berger, 1978 using the software Analyseries, Paillard et al., 1996). Pink bands identify the periods when JJA insolation values at 20° N are below the 470 W/m^2 threshold values (after deMenocal et al., 2000b). Grey bands delineate the warm interglacial periods (marine isotopic stages) and black arrows locate the major isotopic events after Martinson et al., 1987.

value of 470 W/m^2 in the boreal summer (JJA) average insolation, as a threshold which defines humid (insolation above 470) versus arid (insolation below 470) climatic conditions over Africa. Those thresholds are indicated by pink bands in Fig. 5 which underline periods of arid conditions (after deMenocal et al., 2000b). These periods correspond also to precession maxima. Concomitantly, our marine sequence tends to record high Ti/Al ratio, i.e. high dust supply, high residual $\delta^{18}O$ values indicative of high SSS, and SSTs which are systematically above the mean glacial value of 17 °C.

Sedimentological and sea-surface conditions off Mauritania seem then to respond comprehensively to changes which have affected the West African continent over the last 220 ka. At present, such a coupling is coherent with the existence of strong regional teleconnection mechanisms throughout the atmospheric hydrological cycle which is driven by monsoonal phenomena (e.g. Chang et al., 1997; Jury and Mpeta, 2005). During the late Quaternary, feedbacks of surface ocean temperature–moisture transport, together with vegetation–albedo, were already identified as key elements in climate transitions in the area (deMenocal et al., 2000a,b). Over the last climatic cycle, part of the changes observed in past sea-surface conditions off Mauritania (including the upwelling dynamics) was thought to be coherent at the scale of the northern hemisphere climate and promoted by the latitudinal displacement of water masses driven by intertropical and extratropical (polar) climate forcings (e.g. Mittelstaedt, 1983, 1991; Thiede, 1975, 1983; Prell and Curry, 1981; Sarnthein et al., 1982; Ganssen and Sarnthein, 1983; Wefer et al., 1983; Prell, 1984; Sarnthein et al., 1988; Martinez et al., 1999; deMenocal et al., 2000a, 2000b; Ziegler et al., 2008; Itambi et al., 2009). ITCZ migrations along the margin and over the continent were systematically pointed out to explain these environmental changes (e.g. deMenocal, 1995; Martinez et al., 1999; Broccoli et al., 2006; Jullien et al., 2007; Itambi et al., 2009). At the millennial scale, perturbations of the AMOC were furthermore considered as major forcing factors on NW African climates (e.g. Mulitza et al., 2008; Itambi et al., 2009). Results which we obtained for the last 220 ka achieve part of the same finding. However, the proxies (and associated reconstructions) we focussed on, offer the possibility to extensively discuss intrinsic processes linked to the regional ocean dynamics itself.

6.1.1. Upwelling dynamics

At present, geostrophic flows have a strong influence on the regional hydrography off Mauritania. They are expressing themselves powerfully through the dynamics of dominant surface currents and of the adjacent upwelling (see Section 2.2). Variations of the upwelling intensity can be tracked by SST changes, both at modern (e.g. Barton

et al., 1998) and Quaternary scales (e.g. deMenocal et al., 2000a,b), with low SST characterising an increased upwelling activity. According to our results, upwelling is thus preferentially enhanced during (pleni)-glacial times. This is, however, a simplistic view, which does not integrate the latitudinal migration of water masses which accompany glacial/interglacial shifts.

Planktonic foraminifera assemblages bring specific information related to the trophic quality of water masses. For example, high abundances of *G. bulloides* are classically associated in the literature with nutrient-rich environments and upwelling areas (Thiede, 1975, 1983; Prell and Curry, 1981; Ganssen and Sarnthein, 1983; Wefer et al., 1983; Prell, 1984; Naidu, 1990; Thiede and Jünger, 1992; deMenocal et al., 2000a; Meggers et al., 2002; Kuroyanagi and Kawahata, 2004). Its distribution in modern sediments of the area (Fig. 6b after Pflaumann et al., 1996) shows a pattern with maximum abundances recorded directly off Cape Blanc, and at the southern limit of the perennial upwelling (Herbland et al., 1983, see also Fig. 1). Focussing on glacial times, during which maximum abundances of this species are recorded (Figs. 3 and 6), an evolution of the upwelling activity could be drawn from our record. Lowest SST values are recorded during the second half of glacial periods (from to 150 to 130 ka within MIS6, during the whole MIS2, Fig. 6). They coincide with maximum abundances of *G. bulloides* coupled to high absolute foraminifera abundances in sediments (number of shells per gramme of dry sediment) and are furthermore synchronous to high Ti/Al ratios indicative of high dust supplies to the ocean. Intense winds, comparable to the modern Harmattan (i.e. Tulet et al., 2008) seem then to have prevailed during phases of maximum upwelling activity. This is coherent with scenarios of ITCZ migrations, which accompany glacial/interglacial changes, with, a southward shift of the ITCZ during glacials (type of winter monsoon) which permits winds to blow over the area and thus favour upwelling (e.g. deMenocal, 1995; Martinez et al., 1999; Jullien et al., 2007; Itambi et al., 2009).

Regarding the marginal position of our site from the modern upwelling centre (Fig. 1), we further suggest that an extension/migration of the upwelling centre should have occurred during glacials (e.g. Zhao et al., 2000). Indeed, the western African margin upwelling includes at present several latitudinal sub-areas where the upwelling intensity changes seasonally (Navarro-Pérez and Barton, 2001; Aristegui et al., 2009). At least for our area of interest, two domains are distinguishable: a permanent zone (namely the Mauritanian upwelling) between Cape Blanc and Cape Jubi, and a seasonal zone that enlarges the upwelling area up to Cape Verde during winter (Fig. 1). The installation of a winter-like situation during glacials (with a potential migration of the trade wind belt) could have induced a southward expansion of the permanent upwelling zone, thus favouring higher abundances of *G. bulloides* at our site.

We propose that, as a feedback, the changes in the geographical extension and intensity of the upwelling throughout time could modify the climate on the adjacent continent, especially regarding the aridity/humidity balance. Actually, according to previous work along the margin, focused on the last glacial millennial variability, phases of high dust supply to the ocean support the occurrence of NW African droughts forced by southward shift of the West African monsoon trough in conjunction with an intensification and southward expansion of the mid-tropospheric African Easterly Jet (Mulitza et al., 2008). Our observations over the last two glacial cycles suggest continental droughts accompanied by intense upwelling activity. Enhanced/larger upwelling would have favoured increased planktonic productivity. This productivity change could have also been supported by dust advection as a source of macro- and micronutriments to the ocean (e. g. Jickells et al., 2005).

Other remarkable features observed on the basis of foraminifera assemblages (Fig. 6) could help to complete the upwelling dynamics scenario. A look at the evolution of *G. inflata* abundances reveals a specific pattern which could be linked to changes in upwelling (Fig. 6). High percentages of this species are systematically recorded not only during glacial/interglacial shifts, most obvious at Termination 1 (with a peak centred on 14 ka) and Termination 2 (with a peak centred on 128 ka), but also at the onset and termination of MIS6.5 (between isotopic events 6.5 and 6.4, Martinson et al., 1987) during which more discrete peaks are recorded. Such a finding was also evidenced at the proximal ODP site 658 during Termination 1 (e.g. Haslett and Smart, 2006). In the North Atlantic Ocean, *G. inflata* is known to be a transitional species associated with warmer Gulf Stream waters near 18 °C (e.g. Kipp, 1976; Salgueiro et al., 2008). This species is also abundant in non stratified environments (Bé and Tolderlund, 1971). Its distribution in modern sediments of the area (Fig. 6b) shows maximum abundances along the offshore boundary of the permanent upwelling zone. This pattern opposes *G. inflata* to *G. bulloides*, which instead shows high abundances in coastal domains.

The offshore boundary of the modern Mauritanian upwelling is associated with numerous mesoscale structures, known to transfer biogenic material seaward (Barton et al., 1998; Hernandez-Guerra et al., 2005). Strong cyclonic eddies drift slowly southwestward all the yearlong from the Canary archipelago, where they are initiated due to topographic disturbances of the CC (Barton et al., 2004). At present, they define a rich planktonic community that differs from those of the typical coastal upwelling area (Barton et al., 1998). This is what is probably illustrated in the distribution maps of *G. inflata* versus *G. bulloides* in modern sediments (Fig. 6, Pflaumann et al., 1996).

G. inflata abundances >30%, recorded at glacial Terminations in our record, could then be interpreted in two ways: (1) indicating a most active mesoscale dynamics, with numerous eddies reaching our core site, or (2) typifying the prevalence of low-stratification conditions maybe in relation with an expansion of the upwelling area (e.g. Haslett and Smart, 2006). The second hypothesis should support a synchronous increase of *G. bulloides* abundances. However, we observe that *G. inflata* peaks are out of phase and rather follow (or precede) *G. bulloides* optimal occurrence periods. Low stratification conditions in the area are classically attributed to the breakdown of the thermocline due to intense upwelling and trade winds (Hernandez-Guerra et al., 2005). We have shown that during glacials, these situations occur preferentially during megadrought episodes. During the last two glacial periods (Fig. 6), high *G. inflata* percentages are correlated to low Ti/Al ratios, i.e. to humid phases on the continent. The influence of the mesoscale dynamics is thus probably a better candidate to explain variations in the abundances of *G. inflata* in our record. Highest proportions of this species in the planktonic foraminifera assemblages apparently occur not only during major sea-level changes, but also when the permanent upwelling centre moves northward, in response to the poleward migration of the ITCZ, itself driven by global warming which characterises glacial terminations. This mimics the modern ITCZ summer shift with the onset of the rainy season (summer monsoon).

6.1.2. The significance of salinity changes over the area

Our approach allowed reconstructing the residual sea-surface $\delta^{18}O$, which constitutes an indicator of sea-surface salinity (SSS) variations (e.g. Malaizé and Caley, 2009). The record of this SSS estimation through the last 220 ka constitutes a new and original document of the long term evolution of sea-surface conditions off Mauritania. So far, most of the oceanographic and paleoceanographic studies in the area have been focussed on SST variations, picturing the ocean as a vapour source first. Our results thus provide a most complete picture of surface ocean conditions that is worth to be discussed in the light of regional climate changes.

As previously documented in Section 6.1, high residual $\delta^{18}O$ values (i.e. high salinities) occur concomitantly to high dust supply to the ocean during arid phases over the continent (470 W/m^2 insolation threshold, Figs. 5 and 6). Conversely, low residual $\delta^{18}O$ values (i.e. low salinities)

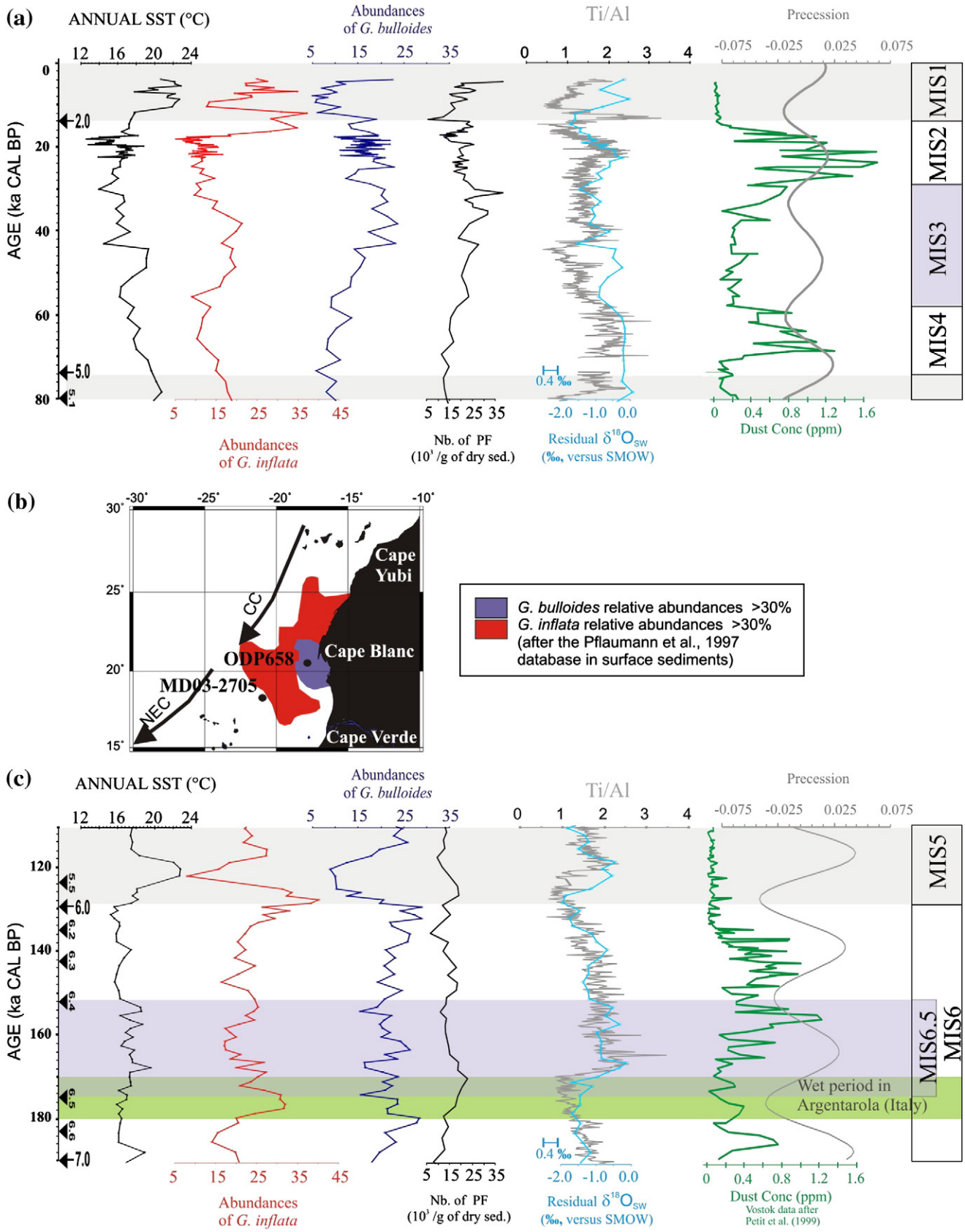

Fig. 6. Compared sea-surface condition evolutions through the last (a) and the penultimate (c) glacial periods regarding some selected proxies in the core MD03-2705: annual SST derived from planktonic foraminifera assemblages, *G. bulloides* and *G. inflata* relative abundances (with (b) a reference to their modern distribution map in regional surface sediments after the database from Pflaumann et al., 1996), absolute concentration of planktonic foraminifera in the sediment, Ti/Al and the residual $\delta^{18}O_{SW}$. These data are compared to the atmospheric dust concentration record from Vostok (after Petit et al., 1999) and to the precession index variations. Grey bands delineate the warm interglacial periods (marine isotopic stages). Black arrows locate the major isotopic events after Martinson et al. (1987). The purple band underlines the MIS6.5 period. The green band identifies the MIS6 wet period in the Argentarola speleothem (after Bard et al., 2002).

are preferentially recorded during low dust supplies corresponding to humid phases (470 W/m^2 insolation threshold, Figs. 5 and 6). The coincidence of high salinities and high dust supplies seems to be driven by boreal-derived influences, i.e. "boreal winter-like" migration of the ITCZ and the intensification of trade winds (past "megadrought" after Mulitza et al., 2008). On the opposite, events of low salinity raise the question of potential fresh water dilution at the surface ocean. This questioning is further justified by previous paleoceanographic results obtained along the African margin (Mulitza et al., 2008; Itambi et al., 2009), which have documented reduced fluvial discharge from the Senegal River during NW African droughts. Does our record indicate similar changes? Could we envisage advection of low salinity plumes from proximal rivers? Which processes permit these events, if any, to be recorded on the MD03-2705 site?

Mechanisms behind the advection of fresh waters may imply a northward migration of water masses and thus variations in the strength of local surface currents, with a possible seesaw between southward and northward directed flows. At present, the latitudinal migration of the Cape Verde Frontal Zone (CVFZ), located close to our studied site (Aristegui et al., 2009, see also Section 2.2), balances North Atlantic central water versus South Atlantic central water (SACW) protrusions. Part of this dynamics directly relates to the CC dynamics. SACW water masses are known to be characterised by low salinity (e.g. Hernandez-Guerra et al., 2005). A northward displacement of the CVFZ, could then explain by itself low salinities over the area. Superimposed, a large influence of Sahelian river discharges could have been favoured at that time. Regarding our record, such a pattern occurred during "humid" African phases, thus in the configuration of summer-like monsoons, when the ITCZ moves northward. Such salinity changes along the last 220 ka are probably further connected to the rate of heat and salt transfers in between the Indo-Pacific and the Atlantic oceans at the southern limb of the African continent (e.g. de Ruijter et al., 1999). Actually, at present, this rate governs the global thermohaline budget and has been evocated as commanding past climate transitions with arguments supporting a teleconnection with the monsoon system (e.g. Peeters et al., 2004; Bard and Rickaby, 2009).

6.2. The atypical MIS6.5 interval off Mauritania

The penultimate glacial period includes the atypical warm substage MIS6.5 (175 ka BP to 152.6 ka BP sensu Martinson et al., 1987), during which interglacial conditions and atypical monsoons were recorded over the subtropics (Rossignol-Strick, 1983; Gasse, 2000; Rossignol-Strick and Paterne, 1999; Masson et al., 2000; Malaizé et al., 2006; Tisserand et al., 2009). As shown in Figs. 4 and 6, peculiar sea-surface conditions were recorded off Mauritania during the MIS6.5 sub-stage compared to the whole MIS6. Higher abundances of tropical species and a nearly 2 °C warming were recorded and are synchronous to high residual δ^{18}O values, which, according to the present SSS–δ^{18}O relationship, could equal modern SSS values. The high SSTs are coherent with what is classically known about this period, but the residual δ^{18}O/salinity and dust signals raise interesting questions. Indeed, regarding our data, the MIS6.5 records the highest salinities and highest dust fluxes of the last 220 ka (Fig. 6). Along the previous discussion sections, we attributed this peculiar feature to drought events, imposed by the extreme equatorward migration of the ITCZ. Here is thus raised the question of the classical humid character attributed to the MIS6.5 period which, obviously, is not the one we noted on the basis of our results. In fact, several phases which reflect distinct climatic states within MIS6.5 could be evidenced from our data. As shown in Figs. 5 and 6, the threshold values of 470 W/m^2 (deMenocal et al., 2000b) were exceeded twice during MIS6 leading to two "humid" events which bracket the MIS6.5 period. These events are coherent with those detected within the δ^{18}O Soreq Cave speleothem record in Israel (Ayalon et al., 2002), which reflect two periods of high precipitation, respectively at the Martinson event 6.5 (175 ky BP) and 6.4 (152 ky BP). For the oldest event, between 175 and 168 ka, proxies from our record indicate a humid phase, with low salinities at the MD03-2705 site and low dust supply at the regional scale, also coherent with the global dust record (Vostok record). This period is also synchronous to a wet event identified in Italy through the Argentarola speleothem record (Bard et al., 2002), and to the deposition of an organic-rich layer (sapropel) in the Eastern Mediterranean, typifying the installation of lowest salinities in this basin due to increasing Nile discharge (Rossignol-Strick, 1983; Kallel et al., 2000; Bard et al., 2002). According to our records, this phase is followed by a sharp increase in dust fluxes and salinities which reach their maximum concomitantly at 166 ka. At the same time, the first large global pulses of atmospheric dust are recorded as depicted by the Vostok ice-core record (Petit et al., 1999). This prominent event is interrupted by a decrease both in dust supply (Tisserand et al., 2009) and salinity (this study) between 165 and 160 ka. In between 158 and 152 ka, evidences of a return to high salinities over the site are registered, coincident with high dust loading both at regional and global scales. The 6.4 isotopic event then records low salinities with progressively decreasing dust fluxes. The coupling observed between dust and salinities proxies during the whole MIS6.5 period is particularly interesting. As previously seen, sea-surface salinities over the MD03-2705 site are probably partly driven by changes in the CFZV dynamics in response to extra- and intra-tropical forcings (see Section 6.1.2). Regarding the close connection with climatic contexts recorded in the Mediterranean region, we can furthermore infer a potential role of this basin as a feedback. Actually, during Mediterranean low salinity events, the influence on site of the intermediate Mediterranean waters in the Canary basin should have been reduced, possibly allowing northward migration of the SACW and low salinity conditions.

7. Conclusion

The analyses conducted on the topmost 11 m of core MD03-2705, have provided a record of past sea-surface conditions over the western African margin during the last 220 kyr. Our approach, relying on qualitative (planktonic foraminifera assemblages, stable isotope and XRF measurements) and quantitative (SST, residual $\delta^{18}O_{SW}$ indicative of past SSS) data, evidences good coherency between surface ocean changes and changes in humidity over the adjacent African continent. Following modelling experiments (e.g. Sepulchre et al., 2009), modern observations (e.g. Jury and Mpeta, 2005; Keenlyside and Latif, 2007), and shorter paleoceanographical records (e.g. deMenocal et al., 2000a; Mulitza et al., 2008; Tisserand et al., 2009), our study thus provides further geological arguments of coupled continental–oceanic forcings on the tropical climate of this area. Contrasting climatic contexts (interglacial versus glacial) indicate changes in the dynamics and in the properties of sea-surface water masses, including modification of the upwellling activity with a probable displacement (or extension) of its permanent centre. These changes occurred concomitantly to latitudinal ITCZ migrations. Higher SSS are recorded over the area during arid intervals and were tentatively interpreted as signing a southward shift of the Cape Verde Frontal Zone. A detailed coupling between dust advection and SSS values over the site of study was noted during MIS6.5.

The identified oceanic variability could be interpreted as reflecting a balance in between extra-tropical forcings, then carrying a strong hemispheric signature (northern versus southern). They are however related to intra-tropical processes, especially throughout the dominant role of moisture exchanges and the hydrological budget.

Acknowledgments

The authors would like to thank all the participants of the scientific cruise PICABIA along with the captains and the crews of the R/V

Marion Dufresne, supported by the French agencies: Ministère de l'Education Nationale de la Recherche et de la Technologie (MENRT), Centre National de la Recherche Scientifique (CNRS), and Institut Paul Emile Victor (IPEV). We are grateful to Olivier Ther for the preparation of the samples and to Clyde Mc Millan for the review of the language. We thank Ralf Schiebel and an anonymous reviewer for their constructive reviews. F. E., B.M., F.G., acknowledge financial support from the French INSU programmes "ECLIPSE" and "LEFE/EVE" (MOMIES project). This is UMR/EPOC CNRS 5805 contribution n°1805.

References

Aristegui, J., Barton, E.D., Alvarez-Salgado, X.A., Santos, A.M.P., Figueiras, F.G., Kifani, S., Hernandez-Leon, S., Mason, E., Machu, E., Demarcq, H., 2009. Sub-regional ecosystem variability in the Canary Current upwelling. Prog. Oceanogr. 83 (1–4), 33–48.

Ayalon, A., Bar-Matthews, M., Kaufman, A., 2002. Climatic conditions during marine oxygen isotope stage 6 in the eastern Mediterranean region from the isotopic composition of speleothems of Soreq Cave, Israel. Geology 30, 303–306.

Bard, E., 1998. Geochemical and geophysical implications of the radiocarbon calibration. Geochimica Cosmochimica Acta 62, 2025–2038.

Bard, E., Rickaby, R., 2009. Migration of the Subtropical Front as a modulator of glacial climate. Nature 406, 380–383.

Bard, E., Delaygue, G., Rostek, F., Antonioli, F., Silenzi, S., Schrag, D.P., 2002. Hydrological conditions over the western Mediterranean basin during the deposition of the cold sapropel 6 (ca. 175 kyr BP). Earth Planet. Sci. Lett. 202, 481–494. doi:10.1016/S0012-821X(02)00788-4.

Barton, E.D., Aristegui, J., Tett, P., Canton, M., Garcia-Braun, J., Hernandez-Leon, S., Nykjaer, L., Almeida, C., Almunia, J., Ballesteros, S., Basterretxea, G., Escanez, J., Garcia-Weill, L., Hernandez-Guerra, A., Lopez-Laatzen, F., Molina, R., Montero, M.F., Navarro-Perez, E., Rodriguez, J.M., van Lenning, K., Velez, H., Wild, K., 1998. The transition zone of the Canary Current upwelling region. Prog. Oceanogr. 41, 455–504.

Barton, E.D., Aristegui, J., Tett, P., Navarro-Perez, E., 2004. Variability in the Canary Islands area of filament–eddy exchanges. Prog. Oceanogr. 62, 71–94.

Bé, A.W.H., 1977. An ecological, zoological and taxonomic review of recent planktonic foraminifera. In: Ramsay, A.T.S. (Ed.), Oceanic Micropaleontology 1. Academic Press, London, p. 100.

Bé, A.W.H., Huston, H.H., 1977. Ecology of planktonic foraminifera and biogeographic patterns of life and fossil assemblages in the Indian Ocean. Micropaleontology 23, 369–414.

Bé, A.W.H., Tolderlund, D.S., 1971. Distribution and ecology of living planktonic foraminifera in surface waters of the Atlantic and Indian oceans. In: Funnell, B.M., Riedel, W.R. (Eds.), Micropaleontology of the Oceans. Cambridge Univ. Press, London, pp. 105–149.

Berger, A., 1978. Long term variation of daily insolation and quaternary climatic change. J. Atmos. Sci. 35, 2362–2367.

Boyle, E.A., 1983. Chemical accumulation variations under the Peru current during the past 130 kyr. J. Geophys. Res. 88, 7667–7680.

Broccoli, A.J., Dahl, K.A., Stouffer, R.J., 2006. Response of the ITCZ to northern hemisphere cooling. Geophys. Res. Lett. 33, L01702. doi:10.1029/2005GL024546.

Chang, P., Ji, L., Li, H., 1997. A decadal climate variation in the tropical Atlantic Ocean from thermodynamic air–sea interactions. Nature 385, 516–518.

Craig, H., Gordon, L.I., 1965. Deuterium and oxygen 18 variations in the ocean and the marine atmosphere. In: Tongiorgi, E. (Ed.), Stable Isotopes in Oceanographic Studies and Paleotemperatures. Consiglio Nazionale di Ricerche, Pisa, Italy, pp. 9–130.

De Ruijter, W.P.M., Biastoch, A., Drijfhout, S.S., Lutjeharms, J.R.E., Matano, R.P., Pichevin, T., Van Leeuwen, P.J., Weijer, W., 1999. Indian–Atlantic interocean exchange: dynamics, estimation and impact. J. Geophys. Res. 104, 20885–20910.

deMenocal, P.B., 1995. Plio-Pleistocene African climate. Science 270 (5233), 53–59. doi:10.1126/science.270.5233.53.

deMenocal, P.B., 2004. African climate change and faunal evolution during the Pliocene–Pleistocene. Earth Planet. Sci. Lett. 220, 3–24. doi:10.1016/S0012-821X(04)00003-2.

deMenocal, P., Ortiz, J., Guilderson, T., Sarnthein, M., 2000a. Coherent high- and low-latitude climate variability during the Holocene warm period. Science 288, 2198–2202.

deMenocal, P., Ortiz, J., Guilderson, T., Adkins, J., Sarnthein, M., Baker, L., Yarusinsky, M., 2000b. Abrupt onset and termination of the African humid period: rapid climate responses to gradual insolation forcing. Quat. Sci. Rev. 19, 347–361. doi:10.1016/S0277-3791(99)00081-5.

Duplessy, J.C., Labeyrie, L.D., Juillet-Leclerc, A., Maitre, F., Duprat, J., Sarnthein, M., 1991. Surface salinity reconstruction of the North Atlantic ocean during the last glacial maximum. Oceanol. Acta 14, 311–324.

Epstein, S., Buchsbaum, R., Lowenstam, H.A., Urey, H.C., 1953. Revised carbonate–water isotopic temperature scale. Geol. Soc. Am. Bull. 64, 1315–1325.

Eynaud, F., unpublished data, in reference to: Eynaud, F., Combourieu-Nebout, N., Malaizé, B., Gouzou, J., Caillon N., Dewilde, F., 2009. Infra-millennial changes in the sea surface temperature of the Alboran Sea during the last 15 Cal-ka: planktonic foraminifera evidences, TMS meeting, June 09, p 31.

Faye, S., Sow, B.A., Lazar, A., 2009. Simulation of the Mauritanian upwelling: how are the winds actually driving SST variability and watermass renewal. Third international AMMA (African monsoon Multidisciplinary Analysis) Conference, July 20–24, Ouagadougou, Burkina Fasohttp://biblio.amma-international.org/index.php?action=listCategoryProcess&id=10.

Flower, B.P., Hastings, D.W., Hill, H.W., Quinn, T.M., 2004. Phasing of deglacial warming and Laurentide Ice Sheet meltwater in the Gulf of Mexico. Geology 32, 597–600.

Fontaine, B., Garcia-Serrano, J., Roucou, P., Rodriguez-Fonseca, B., Losada, T., Chauvin, F., Gervois, S., Sijikumar, S., Ruti, P., Janicot, S., 2009. Impacts of warm and cold situations in the Mediterranean basins on the West African monsoon: observed connection patterns (1979–2006) and climate simulations. Climate Dyn. 1–20. doi:10.1007/s00382-009-0599-3.

Ganssen, G., Sarnthein, M., 1983. Stable isotope composition of foraminifers: the surface and bottom water record of coastal upwelling. In: Suess, E., Thiede J. (Eds.), Coastal Upwelling. Its Sediment Record. Part A: Responses of the Sedimentary Regime to Present Coastal Upwelling. NATO Conference Series, Series IV: Marine Science 10a, Plenum Press, New York, London, 99–121.

Gasse, F., 2000. Hydrological changes in the African tropics since the Last Glacial Maximum. Quat. Sci. Rev. 19, 189–211. doi:10.1016/S0277-3791(99)00061-X.

Gouriou, Y., 1993. The environment in the Eastern Tropical Atlantic. In: Fonteneau, A., Marcille, J. (Eds.), Resources, Fishing and Biology of the Tropical Tunas of the Eastern Central Atlantic. : FAO Fish. Tech. Pap., 292. FAO, Rome, pp. 11–30.

Guiot, J., de Vernal, A., 2007. Transfer functions: methods for quantitative paleoceanography based on microfossils. In: Hillaire-Marcel, C., de Vernal, A. (Eds.), Developments in Marine Geology. : Proxies in late Cenozoic Paleoceanography, 1. Elsevier, Amsterdam, The Netherlands, pp. 523–563.

Hagen, E., 2001. Northwest African upwelling scenario. Oceanol. Acta 24, 113–128.

Hall, N.M.J., Peyrillé, P., 2006. Dynamics of the west African monsoon. J. Phys. IV 139, 81–99.

Harrison, S.P., Kohfeld, K.E., Roelandt, C., Claquin, T., 2001. The role of dust in climate changes today, at the last glacial maximum and in the future. Earth Sci. Rev. 54, 43–80.

Haslett, S.K., Smart, C.W., 2006. Late Quaternary upwelling off tropical NW Africa: new micropalaeontological evidence from ODP Hole 658C. J. Quatern. Sci. 21, 259–269.

Hayes, A., Kucera, M., Kallel, N., Sbaffi, L., Rohling, E.J., 2005. Glacial Mediterranean sea surface temperatures based on planktonic foraminifera assemblages. Quat. Sci. Rev. 24, 999–1016.

Hemleben, Ch., Spindler, M., Anderson, O.R., 1989. Modern Planktonic Foraminifera. Springer-Verlag, New York. 363 pp.

Herbland, A., Le Borgne, R., Le Bouteiller, A., Voituriez, B., 1983. Structure hydrologique et production primaire dans l'Atlantique tropical oriental. Océanogr. Trop. 18, 249–293.

Hernandez-Guerra, A., Fraile-Nuez, E., Lopez-Laatzen, F., Martınez, A., Parrilla, G., Velez-Belchi, P., 2005. Canary Current and North Equatorial Current from an inverse box model. J. Geophys. Res. 110, C12019. doi:10.1029/2005JC003032.

Holz, C., 2004. Climate-induced variability of fluvial and aeolian sediment supply and gravity-driven sediment transport off northwest Africa. Ph.D. dissertation, Univ. of Bremen, Bremen, Germany, 129 pp.

Husar, R.B., Prospero, J.M., Stowe, L.L., 1997. Characterization of tropospheric aerosols over the oceans with the NOAA advanced very high resolution radiometer optical thickness operation product. J. Geophys. Res. 102, 16889–16909.

Itambi, A.C., von Dobeneck, T., Mulitza, S., Bickert, T., Heslop, D., 2009. Millennial-scale northwest African droughts related to Heinrich events and Dansgaard-Oeschger cycles: evidence in marine sediments from offshore Senegal. Paleoceanography 24, PA1205. doi:10.1029/2007PA001570.

Jickells, T.D., An, Z.S., Andersen, K.K., Baker, A.R., Bergametti, G., Brooks, N., Cao, J.J., Boyd, P.W., Duce, R.A., Hunter, K.A., Kawahata, H., Kubilay, N., laRoche, J., Liss, P.S., Mahowald, N., Prospero, J.M., Ridgwell, A.J., Tegen, I., Torres, R., 2005. Global iron connections between desert dust, ocean biogeochemistry, and climate. Science 308, 67–71.

Jullien, E., Grousset, F., Malaizé, B., Duprat, J., Sanchez-Goni, M.F., Eynaud, F., 2007. Low-latitude "dusty events" vs. high-latitude "icy Heinrich events". Quatern. Res. 68, 379–386.

Jury, M.R., Mpeta, E.J., 2005. The annual cycle of African climate and its variability. Water SA 31, 1–8.

Kallel, N., Duplessy, J.-C., Labeyrie, L., Fontugne, M., Paterne, M., Montacer, M., 2000. Mediterranean pluvial periods and sapropel formation over the last 200, 000 years. Palaeogeogr. Palaeoclimatol. Palaeoecol. 157, 45–58.

Keenlyside, N.S., Latif, M., 2007. Understanding equatorial Atlantic interannual variability. J. Climate 20, 131–142.

Kennett, J.P., Srinivasan, M.S., 1983. Neogene Planktonic Foraminifera. A Phylogenic Atlas. Hutchison Ross Publishing Company, Stroudsburg. 259 pp.

Kipp, N.G., 1976. New transfer function for estimating past sea-surface conditions. In: Cline, R.M., Hays, J.D. (Eds.), Investigation of Late Quaternary Paleoceanography and Paleoclimatology, Geological Society of America, Boulder, CO, pp. 3–42.

Klein, B., Siedler, G., 1989. On the origin of the Azores Current. J. Geophys. Res. 94, 6159–6168.

Knoll, M., Hernandez-Guerra, A., Lenz, B., Lopez Laatzen, F., Machin, F., Müller, T.J., Siedler, G., 2002. The eastern boundary current system between the canary Island and the African coast. Deep Sea Res. II 49, 3427–3440.

Kucera, M., 2007. Planktonic Foraminifera as tracers of past oceanic environments. In: Hilaire-Marcel, C., de Vernal, A. (Eds.), Developments in Marine Geology, Volume 1, Proxies in late Cenozoic ¨Paleoceanography. Elsevier, pp. 213–262. ISBN 13: 9780444527554.

Kucera, M., Weinelt, M., Kiefer, T., Pflaumann, U., Hayes, A., Weinelt, M., Chen, M.-T., Mix, A.C., Barrows, T.T., Cortijo, E., Duprat, J., Juggins, S., Waelbroeck, C., 2005. Reconstruction of sea-surface temperatures from assemblages of planktonic foraminifera: multi-technique approach based on geographically constrained calibration data sets and its application to glacial Atlantic and Pacific Oceans. Quatern. Sci. Rev. 24 (7–9), 951–998 SPEC. ISS..

Kuroyanagi, A., Kawahata, H., 2004. Vertical distribution of living planktonic foraminifera in the seas around Japan. Mar. Micropaleontol. 53, 173–196.
LeGrande, A.N., Schmidt, G.A., 2006. Global gridded data set of the oxygen isotopic composition in seawater. Geophys. Res. Lett. 33, L12604. doi:10.1029/2006GL026011.
Lisiecki, L.E., Raymo, M.E., 2005. A Pliocene–Pleistocene stack of 57 globally distributed benthic $\delta^{18}O$ records. Paleoceanography 20, PA1003. doi:10.1029/2004PA001071.
Llinas, O., Rueda, M.J., Marrero, J.P., Perez-Martell, E., Santana, R., Villagarcia, M.G., Cianca, A., Maroto, L., 2002. Variability of the Antarctic intermediate waters in the northern Canary box. Deep Sea Res. II 3441–3453.
Malaizé, B., Caley, T., 2009. Sea surface salinity reconstruction as seen with foraminifera shells: methods and cases studies. Eur. Phys. J. Spec. Top. 167, 179–190.
Malaizé, B., Joly, C., Vénec-Peyré, M.-T., Bassinot, F., Caillon, N., Charlier, K., 2006. Phase lag between Intertropical Convergence Zone migration and subtropical monsoon onset over the northwestern Indian Ocean during marine isotopic substage 6.5 (MIS 6.5.). Geochem. Geophys. Geosyst. 7, Q12N08. doi:10.1029/2006GC001353.
Martinez, P., Bertrand, P., Shimmield, G., Cochrane, K., Jorissen, F., Foster, J., Dignan, M., 1999. Upwelling intensity and ocean productivity off Cap Blanc (Northwest Africa) during the last 70, 000 yrs: geochemical and micropaleontological evidence. Mar. Geol. 158, 57–74.
Martinson, D.G., Pisias, N.G., Hays, J.D., Imbrie, J., Moore, T.C., Shackleton, N.J., 1987. Age dating and the orbital theory of the Ice Ages: development of a high-resolution 0 to 300,000 year chronostratigraphy. Quatern. Res. 27, 1–29.
Maslin, M.A., Shackleton, N.J., Pflaumann, U., 1995. Surface water temperature, salinity, and density changes in the northeast Atlantic during the last 45,000 years: Heinrich events, deep water formation, and climatic rebounds. Paleoceanography 10, 527–544.
Masson, V., Braconnot, P., Jouzel, J., de Noblet, N., Cheddadi, R., Marchal, O., 2000. Simulation of intense monsoons under glacial conditions. Geophys. Res. Lett. 27, 1747–1750.
Meggers, H., Freudenthal, T., Nave, S., Targarona, J., Abrantes, F., Helmke, P., 2002. Assessment of geochemical and micropaleontological sedimentary parameters as proxies of surface water properties in the Canary Islands region. Deep Sea Res. II 49, 3631–3654.
Mittelstaedt, E., 1983. The upwelling area off northwest Africa: a description of phenomena related to coastal upwelling. Prog. Oceanogr. 12, 307–331. doi:10.1016/0079-6611(83) 90012-5.
Mittelstaedt, E., 1991. The ocean boundary along the northwest African coast: circulation and oceanographic properties at the sea surface. Prog. Oceanogr. 26, 307–355. doi:10.1016/0079-6611(91)90011-A.
Moreno, A., Targarona, J., Henderiks, J., Canals, M., Freudenthal, T., 2001. Orbital forcing of dust supply to the North Canary Basin over the last 250 kyrs. Quat. Sci. Rev. 20, 1327–1339.
Mulitza, S., Prange, M., Stuut, J.-B., Zabel, M., von Dobeneck, T., Itambi, A.C., Nizou, J., Schulz, M., Wefer, G., 2008. Sahel megadroughts triggered by glacial slowdowns of Atlantic meridional overturning. Paleoceanography 23, PA4206. doi:10.1029/2008PA001637.
Naidu, P.D., 1990. Distribution of upwelling index planktonic foraminifera in the sediments of the western continental margin of India. Oceanol. Acta 13, 327–333.
Navarro-Pérez, E., Barton, E.D., 2001. Seasonal and interannual variability of the Canary Current. Sci. Mar. 65, 205–213.
Nicholson, S.E., 2009. A revised picture of the structure of the "monsoon" and land ITCZ over West Africa. Clim. Dynam. 32, 1155–1171.
Niedermeyer, E.M., Prange, M., Mulitza, S., Mollenhauer, G., Schefuß, E., Schulz, M., 2009. Extratropical forcing of Sahel aridity during Heinrich stadials. Geophys. Res. Lett. 36, L20707. doi:10.1029/2009GL039687.
Ostlund, H.G., Craig, H., Broecker, W.S., Spencer, D., 1987. GEOSECS Atlantic, Pacific and Indian Oceans Expeditions: Shorebase Data and Graphics. U.S. Government Printing Office, Washington D.C.
Paillard, D., Labeyrie, L., Yiou, P., 1996. Analyseries 1.0: a Macintosh software for the analysis of geographical time-series. EOS 77, 379.
Peeters, F.J.C., Acheson, R., Brummer, G.-J., de Ruijter, W.P.M., Schneider, R.R., Ganssen, G.M., Ufkes, E., Kroon, D., 2004. Vigorous exchange between the Indian and Atlantic oceans at the end of the past five glacial periods. Nature 430, 661–665.
Petit, J.R., Jouzel, J., Raynaud, D., Barkov, N.I., Barnola, J.M., Basile, I., Bender, M., Chappellaz, J., Davis, J., Delaygue, G., Delmotte, M., Kotyakov, V.M., Legrand, M., Lipenkov, V.Y., Lorius, C., Pépin, L., Ritz, C., Saltzman, E., Stievenard, M., 1999. Climate and atmospheric history of the past 420000 years from the Vostok Ice Core, Antarctica. Nature 399, 429–436.
Peyrillé, P., Lafore, J.P., Redelsperger, J.L., 2007. An idealized two-dimensional framework to study the West African monsoon. Part I: validation and key controlling factors. J. Atmos. Sci. 64 (8), 2765–2782.
Pflaumann, U., Duprat, J., Pujol, C., Labeyrie, L., 1996. SIMMAX: a modern analog technique to deduce Atlantic sea surface temperatures from planktonic foraminifera in deep-sea sediments. Paleoceanography 11, 15–35.
Prell, W.L., 1984. Variation of monsoonal upwelling: a response to changing solar radiation. In: Hansen, J., Takahashi, T. (Eds.), Climate Processes: Sensitivity to Solar Irradiance and CO_2, Fourth Ewing Symposium, AGU, Washington, DC, pp. 48–57.
Prell, W.L., Curry, W.B., 1981. Faunal and isotopic indices of monsoonal upwelling: western Arabian sea. Oceanol. Acta 4, 91–98.
Rea, D.K., 1994. The paleoclimatic record provided by Eolian deposition in the deep sea: the geologic history of wind. Rev. Geophys. 32, 159–195.
Richardson, P.L., McKee, T.K., 1984. Average seasonal variation of the Atlantic equatorial currents from historical ship drifts. J. Phys. Oceanogr. 14, 1226–1238.
Rohling, E.J., 2000. Paleosalinity: confidence limits and future applications. Mar. Geol. 163, 1–11.
Rohling, E.J., Bigg, G.R., 1998. Paleosalinity and $\delta^{18}O$: a critical assessment. J. Geophys. Res. 103, 1307–1318.
Rossignol-Strick, M., 1983. African monsoons: an immediate climate response to orbital insolation. Nature 304, 46–49. doi:10.1038/304046a0.
Rossignol-Strick, M., Paterne, M., 1999. A synthetic pollen record of the eastern Mediterranean sapropels of the last 1 Ma: implications for the time-scale and formation of sapropels. Mar. Geol. 153, 221–237. doi:10.1016/S0025-3227(98)00080-2.
Rowell, D.P., 2003. The impact of Mediterranean SSTs on the Sahelian rainfall season. J. Climate 16, 849–862.
Salgueiro, E., Voelker, A., Abrantes, F., Meggers, H., Pflaumann, U., Loncaric, N., González-Álvarez, R., Oliveira, P., Bartels-Jonsdottir, H., Moreno, J., Wefer, G., 2008. Planktonic foraminifera from modern sediments reflect upwelling patterns off Iberia: insights from a regional transfer function. Mar. Micropaleontol. 66 (3–4), 135–164.
Sarnthein, M., Koopman, B., 1980. Late Quaternary deep sea record on northwest African dust supply and wind circulation. Paleoecol. Afr. 12, 239–253.
Sarnthein, M., Thiede, J., Pflaumann, U., Erlenkeuser, H., Fiitterer, D., Koopmann, B., Lange, H., Seibold, E., 1982. Atmospheric and oceanic circulation patterns off northwest Africa during the past 25 million years. In: von Rad, U., et al. (Ed.), Geology of Northwest African Continental Margin. Springer, Berlin, pp. 545–604.
Sarnthein, M., Pflaumann, U., Ross, R., Tiedemann, R., Winn, K., 1988. Global variations of surface ocean productivity in low and mid latitudes: influence of CO_2 reservoirs of the deep ocean and atmosphere during the last 21,000 years. Paleoceanography 3, 361–399.
Schmidt, G.A., 1999. Error analysis of paleosalinity calculations. Paleoceanography 14, 422–429.
Sepulchre, P., Ramstein, G., Schuster, M., 2009. Modelling the impact of tectonics, surface conditions and sea surface temperatures on Saharan and sub-Saharan climate evolution. C. R. Geosci. 341, 612–620.
Stramma, P., Siedler, G., 1988. Seasonal changes in the North Atlantic Subtropical gyre. J. Geophys. Res. 93, 8111–8118.
Stramma, L., Hüttl, S., Schafstall, J., 2005. Water masses and currents in the upper tropical northeast Atlantic off northwest Africa. J. Geophys. Res. 110, C12006. doi:10.1029/2005JC002939.
Stuiver, M., Reimer, P., Reimer, R.W., 2005. CALIB 5.0.
Thiede, J.E., 1975. Distribution of foraminifera in surface water of a coastal upwelling area. Nature 253, 712–714.
Thiede, J.E., 1983. Skeletal plankton and nekton in upwelling water masses off northwestern South America and northwestern Africa. In: Suess, E., Thiede, J.E. (Eds.), Coastal Upwelling: Its Sedimentary Record, Part A. Plenum Press, New York, pp. 183–208.
Thiede, J., Jünger, B., 1992. Faunal and floral indicators of ocean coastal upwelling (NW African and Peruvian continental margins). In: Summerhayes, C.P., Prell, W., Emeis, K.C. (Eds.), Upwelling Systems: Evolution Since the Miocene: Geol. Soc. London, Spec. Publ., 64 (1992), pp. 47–76.
Tiedemann, R., 1991. Acht millionen jahre klimageschichte von nordwest Afrika und paläozeanographie des angrenzenden Atlantiks: Hochauflösende Zeitreihen von ODP-sites 658–661. Geol.-Palaeontol. Inst. Rep. 46, Univ. of Kiel, Kiel, Germany. 190 pp.
Tiedemann, R., Sarnthein, M., Stein, R., 1989. Climatic changes in the western Sahara: aeolo-marine sediment record of the last 8 million years (site 657–661). Proc. Ocean Drill. Program Sci. Results 108, 241–261.
Tisserand, A., Malaizé, B., Jullien, E., Zaragosi, S., Charlier, K., Grousset, F., 2009. African monsoon enhancement during the penultimate glacial period (MIS6.5–170 ka) and its atmospheric impact. Paleoceanography 24, PA2220. doi:10.1029/2008PA001630.
Tulet, P., Mallet, M., Pont, V., Pelon, J., Boone, A., 2008. The 7–13 March 2006 dust storm over West Africa: generation, transport, and vertical stratification. J. Geophys. Res. 113, D00C08. doi:10.1029/2008JD009871.
Turon, Malaizé, 2003. Rapport scientifique de la mission MD134/PICABIA. Les Rapports de Campagne à la Mer IPEV, Brest. 238 pp.
Van Camp, L., Nykjaer, L., Mittelstaedt, E., Schlittenhardt, P., 1991. Upwelling and boundary circulation off northwest Africa as depicted by infrared and visible satellite observations. Prog. Oceanogr. 26, 357–402. doi:10.1016/0079-6611(91)90012-B.
Vidal, L., Labeyrie, L., van Weering, T.C.E., 1998. Benthic $\delta^{18}O$ records in the North Atlantic over the last glacial period (60–10 kyr): evidence for brine formation. Paleoceanography 13, 245–251.
Waelbroeck, C., Labeyrie, L., Michel, E., Duplessy, J.C., McManus, J.F., Lambeck, K., Balbon, E., Labracherie, M., 2002. Sea-level and deep water temperature changes derived from benthic foraminifera isotopic records. Quatern. Sci. Rev. 21 (1–3), 295–305.
Weaver, P.P.E., Wynn, R.B., Kenyon, N.H., Evans, J., 2000. Continental margin sedimentation, with special reference to the north-east Atlantic margin. Sedimentology 47, 239–256. doi:10.1046/j.1365-3091.2000.0470s1239.x.
Wefer, G., Dunbar, R.G., Suess, E., 1983. Stable isotopes of foraminifers off Peru recording high fertility and changes in upwelling history. In: Thiede, J.E., Suess, E. (Eds.), Coastal Upwelling: Its Sedimentary Record, Part B. Plenum Press, New York, pp. 295–308.
WOA, 1998. World Ocean Atlas 1998. National Oceanographic Data Center, Silver Spring, Maryland. http://www.nodc.noaa.gov/oc5/woa98.html, Extraction tool used: Christian Schäfer-Neth & Andreas Manschke : http://www.geo.uni-bremen.de/geomod/Sonst/Staff/csn/woasample.html.
Zhao, M., Eglinton, G., Haslett, S.K., Jordan, R.W., Sarnthein, M., Zhang, Z., 2000. Marine and terrestrial biomarker records for the last 35,000 years at ODP site 658C off NW Africa. Org. Geochem. 31, 919–930.
Ziegler, M., Nurnberg, D., Karas, C., Tiedemann, R., Lourens, L.J., 2008. Persistent summer expansion of the Atlantic Warm Pool during glacial abrupt cold events. Nat. Geosci. 1, 601–605.